Galectin-3, a Novel Centrosome-associated Protein, Required for Epithelial Morphogenesis

Annett Koch,*† Francoise Poirier,‡ Ralf Jacob,* and Delphine Delacour*§

*Department of Cell Biology and Cell Pathology, Philipps University, D-35033 Marburg, Germany;
‡Jacques Monod Institute, UMR-CNRS7592, Paris Diderot University, 75013 Paris, France

Galectin-3 is a β-galactoside–binding protein widely expressed in all epithelia where it is involved in tissue homeostasis and cancer progression. We recently reported unique abnormalities in the identity of membrane domains in galectin-3 null mutant mice, suggesting that galectin-3 may participate in epithelial polarity program. We investigated the potential role of galectin-3 on early events in polarization of epithelial renal cells, using three-dimensional cultures of MDCK cells and also galectin-3 null mutant mouse kidneys. We show that depletion in galectin-3 systematically leads to severe perturbations of microtubular network associated with defects in membrane compartmentation, both in vitro and in vivo. Moreover, the absence of galectin-3 impinges on the morphology of the primary cilium, which is three times longer and unusually shaped. By immunological and biochemical approaches, we could demonstrate that endogenous galectin-3 is normally associated with basal bodies and centrosomes, where it closely interacts with core proteins, such as centrin-2. However, this association transiently occurs during the process of epithelial polarization. Interestingly, galectin-3–depleted cells contain numerous centrosome-like structures, demonstrating an unexpected function of this protein in the formation and/or stability of the centrosomes. Collectively, these data establish galectin-3 as a key determinant in epithelial morphogenesis via its effect on centrosome biology.

INTRODUCTION

Galectins are a family of proteins that have been initially described for their affinity for β-galactoside motifs (Barondes et al., 1994). They are highly conserved from nematodes to vertebrates, suggesting a central role for these proteins in multicellular organisms (Cooper, 2002). Galectins have been implicated in development, tissue homeostasis, immune response, and tumor progression (Poirier, 2002; Rabinovich et al., 2002; Liu and Rabinovich, 2005). In vivo, their expression profiles vary depending on developmental stage and cell differentiation (Liu et al., 2002; Poirier, 2002). Galectins are small soluble proteins, devoid of signal peptide, that can be secreted by an unconventional, still unknown mechanism (Cooper, 2002; Hughes, 1999; Nickel, 2003, 2005). They can be found in the extracellular medium, but also in different intracellular compartments. As a consequence, they can exert multiple cellular functions. Previous studies, mainly performed in vitro, described their participation in cell/extracellular matrix or cell/cell interactions, in apoptosis, cell cycle and even mRNA splicing (Hughes, 2001; Liu et al., 2002; Elola et al., 2007). In addition to this wide-range of functions already ascribed to galectins, we have established their role in polarized epithelial cells, where they directly

participate in intracellular protein trafficking (Delacour et al., 2005, 2006, 2007, 2009).

Galectin-3 is one of the most extensively studied member of the family. In mammals, it has been detected in macrophages, eosinophils, neutrophils, in sensory neurons, bones, and also in epithelial cells of the gastrointestinal, respiratory, and urogenital tracts (Krzeslak and Lipinska, 2004). We demonstrated that galectin-3 regulates glycoprotein apical trafficking in fully differentiated epithelial cells in vitro and in vivo (Delacour et al., 2006; Delacour et al., 2007; Delacour et al., 2008). Interestingly, the analysis of small intestines from gal3−/− mice revealed that, in addition to intracellular trafficking defects, the cytoarchitecture of epithelial cells is fundamentally altered (Delacour et al., 2008). Hence, the basolateral membranes of gal3−/− enterocytes display characteristic features of apical membranes, with the presence of numerous, organized membrane interdigitations in which apical brush border markers, such as villin or ezrin, abnormally relocalize. We then hypothesized that the role of galectin-3 in intracellular trafficking could not account alone for all the defects that were observed. Instead, the lectin was probably also involved at an earlier stage, in the establishment of cell polarity.

In the present study, we used three-dimensional cultures of Madin-Darby canine kidney (MDCK) cells to analyze early events occurring in the process of epithelial morphogenesis. In parallel, we analyzed adult mouse kidneys, where galectin-3 is specifically expressed in epithelial cells lining distal and collecting ducts (Winyard et al., 1997; Bichara et al., 2006). We show that depletion of this lectin leads to a misorganization of renal epithelial cells both in vitro and in vivo. Concomitant defects in the development of the primary cilium, an unconventional organelle important for epithelial organization in vertebrates (Singla and Reiter, 2006; Fliegauf et al., 2007), were observed in absence

of galectin-3. Interestingly, we found that galectin-3 transiently associates with the centrosomes during the process of polarization and that dramatic centrosomal abnormalities occur in the absence of galectin-3 expression both in MDCK cells and in mouse kidneys. Taken together, our findings strongly suggest a crucial role for the lectin in centrosome biology.

MATERIALS AND METHODS

Materials, Reagents, and Antibodies

Mouse monoclonal antibodies directed against galectin-3, villin, gp114, or gp135 were gifts from Dr. H. Leffler (Lund University, Sweden), Dr. S. Robine (Institut Curie, Paris), Dr. K. Simons (MPI-CBG, Dresden, Germany), and Dr. G. Ojakian (State University of New York Downstate Medical Center, Brooklyn, NY), respectively. Rabbit polyclonal antibodies against galectin-3, ezrin, and centrin-2 or centrin-3 were kindly provided by Dr. H. P. Elsässer (Philipps University, Marburg), Dr. M. Arpin (Institut Curie, Paris), and Dr. M. Bornens (Institut Curie, Paris), respectively. Rabbit anti-centrin-2 antibodies were from Sigma (St. Louis, MO) and from Santa Cruz Biotechnology (Santa Cruz, CA), rabbit anti-pericentrin from Covance (Berkeley, CA), rabbit anti-aquaporin-2 from United States Biological (Swampscott, MA), rabbit anti-Na$^+$/K$^+$-ATPase from Abcam (Cambridge, MA), monoclonal anti-α- and β-tubulin, and anti-acetylated-α-tubulin, or rabbit γ-tubulin were from Sigma and monoclonal anti-flotillin-1 from BD Biosciences (Rockville, MD). Alexa 488, 546, or 633 secondary antibodies were from Molecular Probes (Invitrogen, Eugene, OR). Hoechst 33348 (Fluka, Ronkonkoma, NY) staining was used to detect nuclei.

Mice and Preparation of Tissue Samples

Wild type (wt) and *galectin-3* null mutant (Colnot *et al.*, 1998) mice used in this study were of 129Sv background. The animals were maintained as previously described (Delacour *et al.*, 2008). A total of 31 wt and 31 *gal3*−/− mice from 6 mo to 1 y old have been used along this study.

Kidneys from 12 wt and 12 *gal3*−/− mice were fixed in Carnoy solution (60% ethanol, 30% chloroform, 10% acetic acid) overnight. For centrosome analyses, kidneys from six wt and six *gal3*−/− mice were fixed by successive 1-h incubations in cold 70, 90, and 100% methanol solutions. Samples were paraffin-embedded. For microtubule detection, kidneys from four wt and four *gal3*−/− mice were fixed in 4% PFA for 3 h and then snap-frozen in OCT Tissue-Tek (Sakura Finetek, Zoeterwoude, the Netherland). Paraffin sections (5 μm) or cryosections (10 μm) were prepared for immunohistological analyses.

MDCK Cell Culture, siRNA Transfection

MDCK cells were routinely grown in DMEM 4.5 g/l glucose, 10% FCS, 10% penicillin-streptomycin (PAA Laboratories, Linz, Austria). Culture medium was renewed every day. Cells reach confluency after 2 d of culture, and polarized cells were obtained after 6 d. For 3D cultures, trypsinized MDCK cells were resuspended in pure Matrigel (BD Biosciences) at a final concentration of 2×10^4 cells/ml. Matrigel cell suspension, 30 μl, was laid onto precooled 1.2-mm coverslips. MDCK cysts were grown for 5 d, and medium was daily renewed.

Transfections were done using Lipofectamine 2000 reagent (Invitrogen) following the manufacturer's recommendations. Galectin-3 reduction was carried out as previously described (Delacour *et al.*, 2006) by transfecting a mix of siRNAs duplexes, so called gal3 siRNA, directed against canine galectin-3 (gal3 siRNA a: 5′-AUACCAAGCUGGAUAAAUAUTT-3′/3′-TTUAUG-GUUCGACCUAUUAUA-5′, gal3 siRNA b: 5′-ACCCAAACCCUCAAG-GAUGTT-3′/3′-TTUGGGUUUGGGAGUUCCUAC-5′), purchased from Genordia (Bromma, Sweden). Mock transfections were performed by using luciferase siRNA (Genordia). Specificity of gal3 siRNA was checked by transfecting either an inefficient gal3 siRNA duplex (target sequence: GAAGAAA-GACAGUCGGUUU; Dharmacon, Lafayette, CO), or another competent galectin-3 siRNA, gal3 siRNA#2 (5′-UUGUACUGCAACAAAUGGG-3′/3′-CCCAUUUGUUGCAGUACAA-5′; Invitrogen). Efficiency and specificity of galectin-3 reduction was assessed by Western blot. For 3D cultures, siRNA transfections were first carried out on 2D cultures for 2 d, and cells were then trypsinized and processed for Matrigel suspension. siRNAs were still added in the medium of Matrigel cultures for an additional 2 d.

Centrosome Preparation

The preparation was carried out as described by Bornens and Moudjou (1999). Twenty plates (Ø10 cm) of postconfluent MDCK cells were treated 1.5 h at 37°C with nocodazole (10 μM) and cytochalasin B (5 μM). Cells were rinsed with PBS, scraped, and collected in a tube with PBS. After a first pelleting step, cells were resuspended in 4.5% Nycodenz (Axis-Shield, Oslo, Norway) and pelleted again. After addition of 20 ml of lysis buffer (1 mM Tris/HCl, pH 8.0, 0.1% β-mercaptoethanol [β-ME], 0.5% NP-40, 1 mM PMSF) cells were

resuspended and incubated for 5 min at 4°C. After nuclear sedimentation for 10 min at 1300 $\times$ *g*, the supernatant was supplemented with 1:50 volume of Pipes buffer (0.5 M Pipes/KOH; pH 7.2, 1 mM EDTA, 600 Units DnaseII) and mixed 30 min at 4°C. The suspension was loaded on top of a step-gradient (27-33%-50% Nycodenz in 10 mM Pipes/KOH, pH 7.2, 1 mM EDTA, 0.1% β-ME, 0.1% TX-100) and centrifuged for 1 h at 100,000 $\times$ *g*. Two-milliliter fractions were collected from the top. For pelleting, the fractions were diluted eightfold with 10 mM Pipes, pH 6.9, and centrifuged for 15 min at 40,000 $\times$ *g*. For immunoprecipitation, 400 μl of buffer (50 mM Tris/HCl, pH 8.0, 150 mM NaCl, 1 mM DTT, 0.5% NP-40, 2 mM EGTA) were added to each fraction and incubated for 45 min at 4°C. A preclearing step was achieved by incubating protein A Sepharose (PAS) beads (Sigma). Anti-centrin-2 antibody (Sigma) was applied to precleared fractions. Immunocomplexes were recovered by addition of PAS beads overnight at 4°C. Then three washes were done in lysis buffer. Finally, beads were resuspended in Laemmli buffer for Western blot procedure.

Immunofluorescence and Confocal Fluorescence Microscopy

For classical immunofluorescence, cells grown on solid support or on Matrigel matrix were fixed in 4% PFA for 15 min or 1 h, respectively. Cell permeabilization was done by incubating in 0.025% saponine in PBS and saturation in PBS containing 0.025% saponine, 1% BSA.

For detection of centrosomal structures, immunofluorescence procedure was modified as in Tassin *et al.* (1998). Cells were fixed in −20°C precooled methanol for 6 min. After PBS wash, cell permeabilization was carried out in PHEM buffer (45 mM Pipes, 45 mM HEPES, 10 mM EGTA, 5 mM MgCl$_2$, pH 6.9) containing 0.025% saponine. Primary antibody incubations were performed in PBS containing 0.025% saponine, 1% BSA, at 4°C for 12 h for 2D cultures or 24 h for Matrigel suspensions. Secondary antibodies (Invitrogen) were incubated 1 h for 2D cultures or 12 h for Matrigel suspension. Nuclei were detected by Hoechst 33342 staining (Fluka). Cells were mounted in Mowiol 488 solution (Calbiochem, La Jolla, CA).

Paraffin sections were dewaxed in xylene bath and rehydrated once in isopropanol and in increasing ethanol solutions. Sections were saturated in 10% goat serum (Dako, Carpinteria, CA) for 30 min. Antibody incubations were done at 4°C for 12 h in 10% goat serum solution. The same procedure was used for cryosections, but goat serum was replaced by 1.5% donkey serum (Sigma). Hoechst 33342 staining was used to detect nuclei. Tissue sections were mounted in Mowiol488 solution.

Confocal images of fixed cells were acquired on Leica TCS SP2 and SP5 microscopes using a 63$\times$ and 100$\times$ lens (Leica Microsystems, Deerfield, IL). Quantitative analyses have been processed with Volocity software package (Improvision, Coventry, England) and Lucia image analysis software (Lucia Cytogenetics, Prague, Czech Republic).

Electron Microscopy

For ultrastructural analysis, tissue samples were isolated from six wt and six *gal3*−/− mouse kidneys, cut into small ~1 mm³ pieces and immersion-fixed in 0.05% picric acid in 0.067 M cacodylate buffer, pH 7.4, for 2 h at 4°C. Standard procedures for dehydration and embedding in Epon were used. Three wt and three *gal3*−/− mouse kidneys were processed for immunostaining experiments. Tissue samples were fixed in 1% PFA, 0.1% glutaraldehyde, 0.1M cacodylate buffer, pH 7.4, overnight and then embedded in Lowicryl K4M resin (Polysciences, Warrington, PA). Ultrathin sections were treated with 1% BSA before incubation in anti-centrin-2 antibody (Santa Cruz), followed by 10-nm immunogold-conjugated goat anti-rabbit antibody solution (British Biocell International, Cardiff, United Kingdom). In both cases, thin sections were stained with uranyl acetate and lead citrate before examination using an EM 109 electron microscope (Zeiss, Thornwood, NY) and an EM Tecnai electron microscope (Philipps, Eindhoven, the Netherlands).

RESULTS

Galectin-3 Is Required for Epithelial Organization

To test the role of galectin-3 in the early events of epithelial organization, we used the well-characterized MDCK cell model, in which galectin-3 is known to be highly expressed (Lindstedt *et al.*, 1993). When grown in three dimensions, MDCK cells set their own polarity, which leads to the formation of regular, monolayered, single lumen cysts over a period of 4–5 d (O'Brien *et al.*, 2002; Martin-Belmonte and Mostov, 2008). At the end of this process, the cells are fully polarized with the apical domain facing the lumen as indicated by the distribution of apical plasma membrane–associated proteins, such as gp114 and gp135 (Figure 1A). To test the importance of galectin-3 on MDCK cystogenesis, we compared the effect of siRNA directed against galectin-3
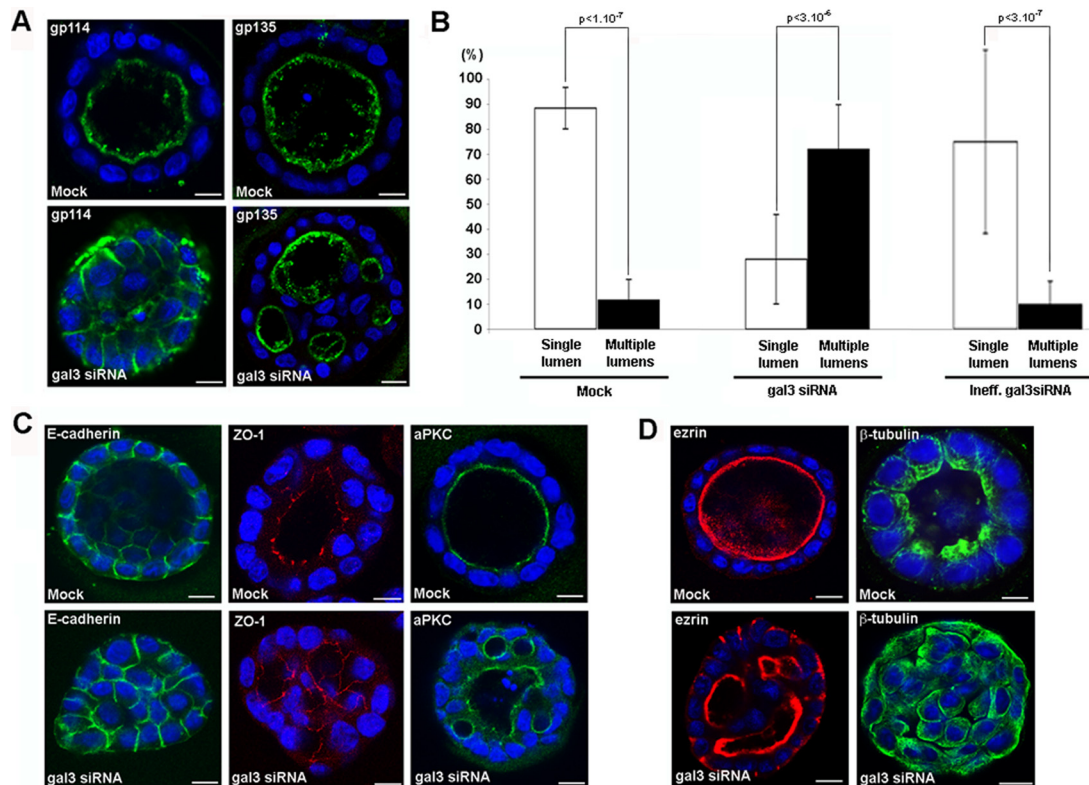
Figure 1. Depletion of galectin-3 leads to abnormal cystogenesis in MDCK cells. MDCK cells were cultured in Matrigel 3D matrix for 5 d. (A) distribution of gp114 and gp135 in control (luciferase siRNA or Mock) or in cells transfected with galectin-3 siRNA (gal3 siRNA). (B) quantification. Controls, i.e., Mock (n = 206) and inefficient gal3 siRNA (n = 114), or galectin-3 siRNA (n = 137) cysts have been analyzed in three independent experiments. Bars, mean ± SD. Mann-Whitney tests have been performed, and statistical differences (p) are presented. Distribution of E-cadherin, ZO-1, aPKC (C), ezrin, and β-tubulin (D), in control (Mock) or in cells transfected with galectin-3 siRNA (gal3 siRNA). Nuclei were detected by Hoechst 33342 staining. Scale bars, 10 μm.

(gal3 siRNA) to that directed against luciferase (Mock) or an inefficient galectin-3 siRNA (Ineff.gal3 siRNA) as a controls (Figure 1A and Supplemental Figure 1B). The reduction in the amount of galectin-3 is presented in Supplemental Figure 1A. In contrast to the control situations, we found profound changes in the distribution of the two apical proteins gp114 and gp135 in galectin-3 siRNA-treated MDCK cells (Figure 1A and Supplemental Figure 1B). On the one hand, the nonraft associated gp114 was relocated along basolateral membrane of cyst cells upon galectin-3 reduction; on the other hand, gp135, a raft-associated protein, was still apically targeted. This specific effect of galectin-3 depletion on raft-independent trafficking is consistent with our previous observations (Delacour *et al.,* 2006, 2007). In addition to these cellular defects, we also observed defects in the organization of the cysts: cells depleted in galectin-3 failed to generate a single, regular, central lumen, and they instead developed cysts with multiple small lumens, which were positive for gp135 (Figure 1A and Supplemental Figure 1B). All these defects were also observed after transfecting with another competent galectin-3 siRNA (Supplemental Figure 2, A and B).

A quantitative comparison revealed that in the control situation, 90% of the cysts display a single lumen, whereas galectin-3 siRNA transfection resulted in the formation of more than 70% abnormal cysts with multiple lumens (Figure 1B). This finding corroborates recent data on the perturbation of epithelial cyst formation after galectin-3 depletion (Torkko *et al.,* 2008), and thus confirms the role of galectin-3 in this cellular process.

To further analyze the polarity of cells surrounding the aberrant lumens, we studied the localization of determinants of epithelial cytoarchitecture. We found that the distribution of the basolateral marker E-cadherin was not affected by galectin-3 reduction (Figure 1C and Supplemental Figure 1C). Similarly, the tight junction component ZO-1 and the atypical protein kinase C (aPKC), a member of the Par3/Par6/aPKC polarity complex (Assemat *et al.,* 2008; Tanos and Rodriguez-Boulan, 2008), were both normally located at the apical domains along each supranumerous lumina (Figure 1C and Supplemental Figure 1C). Together with gp135 distribution, these results show that, upon galectin-3 reduction, bona fide apical and basolateral markers are normally distributed indicating that individual MDCK cells acquire some major characteristics of polarized cells, despite the failure of the cell population to form single lumen cysts.

Defects were however observed after staining for ezrin, a structural component of microvilli (Crepaldi *et al.,* 1997; Bonilha *et al.,* 1999); besides the expected signal along supranumerary lumina, ezrin was also relocated close to basolateral membranes in galectin-3–depleted cysts (Figure 1D, Supplemental Figures 1C and 2C). Furthermore, when we used β-tubulin antibody, we found that depletion in galectin-3 resulted in a systematic profound disorganization of the microtubular network. In control cysts, the microtubule array originates from the apical domain and it runs parallel to the lateral membranes, along the apico-basal axis. After galectin-3 reduction, the cells exhibited an irregular pattern of tubulin staining

with spread out microtubules inside cells, without any apparent organization (Figure 1D, Supplemental Figures 1C and 2C). Altogether, these experiments show that in developing MDCK cell cysts, galectin-3 contributes to epithelial morphogenesis.

In adult mouse kidneys, galectin-3 is specifically expressed in epithelial cells lining distal tubules and collecting ducts, but not in proximal tubules (Winyard *et al.,* 1997; Bichara *et al.,* 2006; Kim *et al.,* 2007). There was already indirect evidence for a role of galectin-3 in epithelial cell morphogenesis in mouse kidneys. First, adult *gal3*−/− mutant mice display renal hypertrophy and an 11% reduction in the total number of nephrons (Bichara *et al.,* 2006). Second, the absence of galectin-3 expression exacerbates the polycystic kidney phenotype in mice (Chiu *et al.,* 2006). Given our results, we thus examined epithelial cell organization in *gal3*−/− collecting ducts. Using confocal microscopy, we analyzed the distribution of apical or basolateral markers on wt (number of mice analyzed n = 12) or *gal3*−/− (n = 12) mouse kidney sections. In comparison to wt cells, the Na^+/K^+-ATPase retained a normal basolateral distribution in most mutant cells (Figure 2A). As expected, the nonraft associated gp114 redistributed along basolateral membranes (Figure 2B), whereas the apical localization of the raft-associated aquaporin-2 (AQ-2; Kamsteeg *et al.,* 2007; Yu *et al.,* 2008) was unchanged (Figure 2C) in *gal3*−/− cells compared with wt cells. Interestingly, the distribution of villin, a microvillus structural component (Revenu *et al.,* 2004) was always profoundly perturbed in the absence of galectin-3. In wt collecting ducts, an intense and regular villin signal was restricted to the apical plasma membranes along the urinary tubules (Figure 2D). In the kidneys of mutant animals, villin distribution was never polarized, it was found in the cytoplasm as well as along the apical and basolateral membranes (Figure 2D). These effects on cell polarity were limited to the collecting duct epithelial cells. No abnormalities in membrane compartimentation were ever noted in mutant proximal tubules (data not shown). When we next compared the organization of microtubule arrays, we found that tubulin bundles originating from the subapical domains were easily detectable in renal cells lining every collecting ducts (n = 4; Figure 2E). In contrast, the tubulin staining was stronger in the cytoplasm, closer to the nuclei than in the subapical domains of galectin-3 null mutant cells (n = 4). As shown in Figure 2E, mutant collecting duct cells displayed an irregular pattern of α-tubulin, suggesting a partial disorganization of the microtubule network in *gal3*−/− collecting ducts. Again, this aberrant distribution of α tubulin was observed in every mutant animal, and proximal tubules were not affected. Altogether, these results point to a central role for galectin-3 in renal epithelial organization, not only in vitro but also in vivo.

Galectin-3 Is Required for Ciliogenesis

The primary cilium is known to play a key role in epithelial morphogenesis during kidney development (Singla and Reiter, 2006; Satir and Christensen, 2008). To test whether the galectin-3 null mutation impinges on primary cilium formation, we performed immunostaining with the antibody directed against the acetylated form of α-tubulin on kidney cells from wt or *gal3*−/− adult mice. As shown in Figure 3A, cilia are small structures located on the apical side of the cells lining the collecting ducts. Surprisingly, we found that all *gal3*−/− cells displayed much longer and irregular cilia, indicating that galectin-3 might modulate the development of the primary cilium. The same observations were made in MDCK cysts (Figure 3B and Supplemental

Figure 2D). To obtain quantitative data on primary cilium formation, we analyzed MDCK cells after 4 d in culture on a solid support. In these conditions it was possible to visualize the entire cilium in the same optical plan. We found that, in comparison to control cells, the growth of the primary cilium was deeply perturbed in galectin-3 siRNA-treated cells (Figure 3C and Supplemental Figure 2E). We observed a systematic increase in cilia length in cells transfected with galectin-3 siRNA. When measured in three independent experiments, the increase was estimated in the order of 3.4-fold in galectin-3 siRNA-treated cells ($p < 1 \times 10^{-7}$; Figure 3D). Additionally, the shape of mutant primary cilia was also affected. Cilia were abnormally bent and curly (Figure 3C and Supplemental Figure 2E; higher magnification on right sides). Occasionally, the primary cilia from neighboring mutant cells even became aberrantly entangled (Figure 3C and Supplemental Figure 2E). These data show that galectin-3 is required for correct development of the primary cilium in renal epithelial cells.

Galectin-3 Is a Transient Centrosomal Component

It is already known that galectin-3 is distributed in the cytoplasm and at the plasma membrane in fully polarized epithelial cells (Liu *et al.,* 2002; Delacour *et al.,* 2008). However, because it is affecting ciliogenesis, we wondered whether it could also be present in the primary cilium. We found that galectin-3 intracellular localization is highly dynamic during MDCK cell differentiation (Supplemental Figure 3A, a–f). At day 0–2, nuclear (a) and/or cytosolic (b) distribution was observed. Unexpectedly, at day 3–4, in postconfluent cells, galectin-3 staining revealed, in addition to the weak cytosolic staining, a strong concentration in z discrete point located either in the perinuclear area (c) or at the apical plasma membrane (d), a pattern consistent with centrosomes or basal bodies. At day 5–7, in fully differentiated MDCK cells, galectin-3 displays a cytosolic and vesicular pattern (e), the major part of galectin-3 signal was detected at the apical cell surface (f), as already reported (Delacour *et al.,* 2007). To characterize galectin-3 distribution in postconfluent MDCK cells, we performed double immunostaining experiments using anti-galectin-3 and anti-acetylated α-tubulin antibodies to visualize primary cilia and acquired pictures using confocal microscopy (Figure 4A). No signal for galectin-3 was observed inside the axonemal part of the cilium, but a single intense and regular spot of galectin-3 signal was indeed revealed at the basis of each individual primary cilium, i.e., at the basal body/mother centriole level. This was further confirmed by colocalization of galectin-3 with centrin-2, a centriolar protein (Laoukili *et al.,* 2000; Figure 4A). Furthermore, this colocalization between galectin-3 and centrin-2 was observed not only at the apical plasma membrane, but also in the cytoplasm, indicating that galectin-3 could be, more generally, associated with the centrosome. We consequently tested the presence of galectin-3 at the centrosome. As shown in Figure 4B, galectin-3 staining inside the cells overlapped with the labeling of centrosomal proteins, such as γ-tubulin and pericentrin (Dictenberg *et al.,* 1998). The localization of galectin-3 at the centrosome/basal body was also observed in MDCK cysts grown in Matrigel (Supplemental Figure 3, B–D) and in mouse kidneys (Supplemental Figure 4).

To confirm the association of endogenous galectin-3 with the centrosome, we next took a biochemical approach. After disruption of cytoplasmic microtubules by nocodazole treatment, centrosomal fractions were prepared from day 3 MDCK cells by discontinuous Nycodenz gradient fractionation (Figure 4C). Fractions were collected from top to bot-
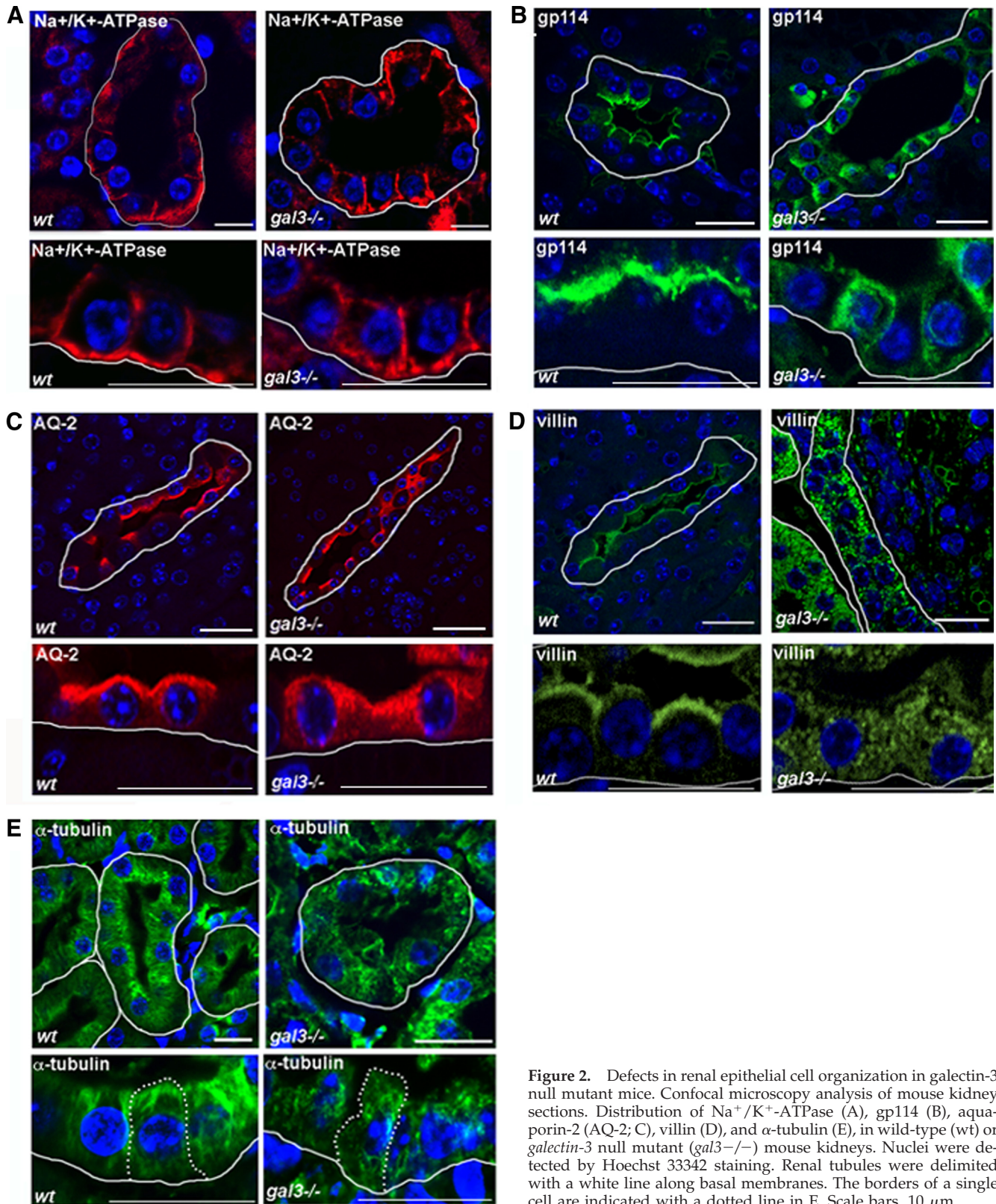
Figure 2. Defects in renal epithelial cell organization in galectin-3 null mutant mice. Confocal microscopy analysis of mouse kidney sections. Distribution of Na$^+$/K$^+$-ATPase (A), gp114 (B), aquaporin-2 (AQ-2; C), villin (D), and α-tubulin (E), in wild-type (wt) or *galectin-3* null mutant (*gal3−/−*) mouse kidneys. Nuclei were detected by Hoechst 33342 staining. Renal tubules were delimited with a white line along basal membranes. The borders of a single cell are indicated with a dotted line in E. Scale bars, 10 μm.

tom and analyzed by Western blot. We first assessed the specificity of the overall procedure. γ-Tubulin and centrin-2 were exclusively present in fractions 10 and 11, whereas noncentrosome-associated proteins such as flotillin-1 were

mainly distributed in fractions 1-9. As shown in Figure 4C, across the entire gradient, the distribution of galectin-3 was similar to that of γ-tubulin and centrin-2, clearly showing the enrichment of galectin-3 at the centrosome in postcon-
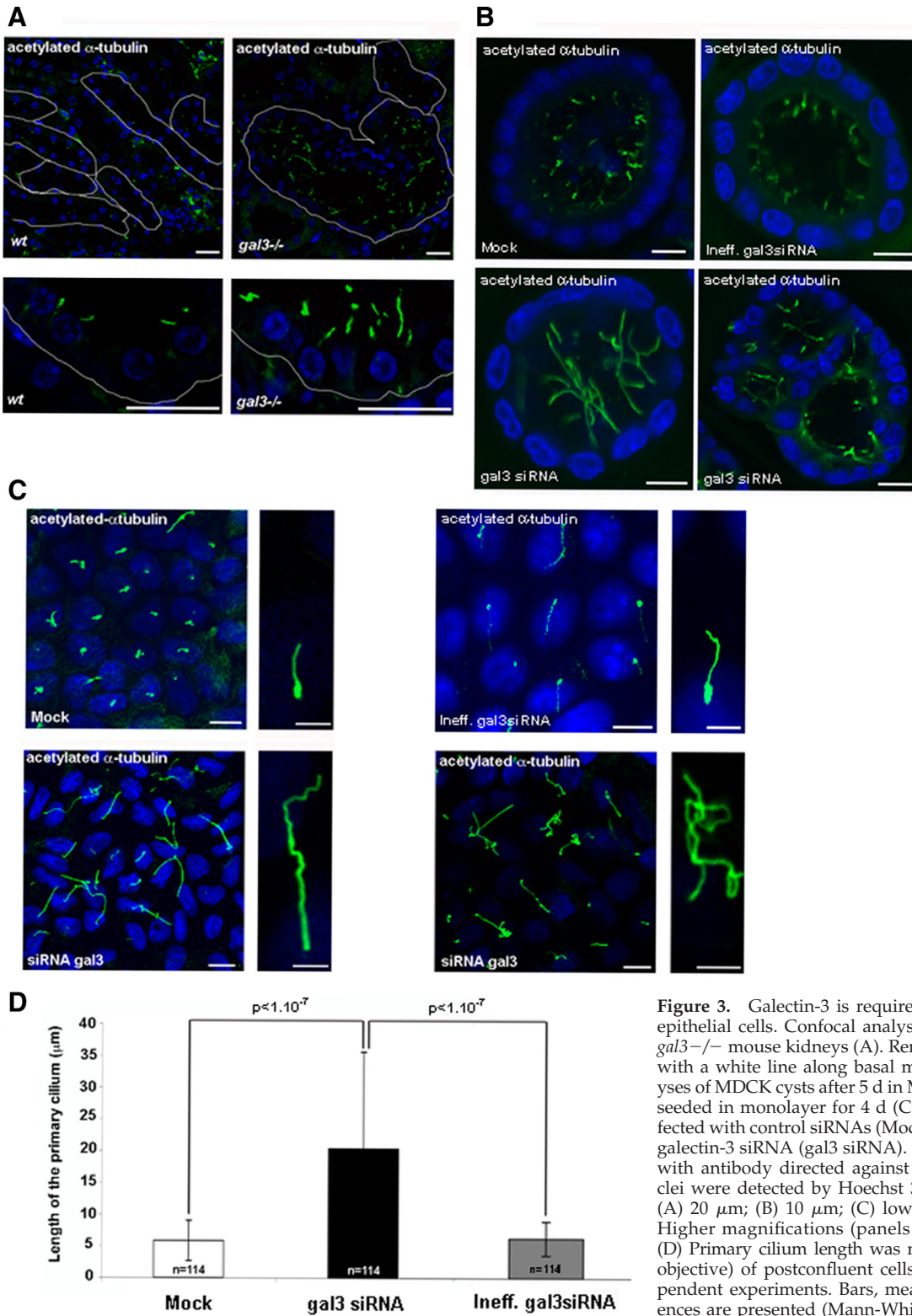
A

B

C

D

Figure 3. Galectin-3 is required for ciliogenesis in renal epithelial cells. Confocal analysis of ciliogenesis in wt or *gal3*−/− mouse kidneys (A). Renal tubules were delimited with a white line along basal membranes. Confocal analyses of MDCK cysts after 5 d in Matrigel (B) or MDCK cells seeded in monolayer for 4 d (C). MDCK cells were transfected with control siRNAs (Mock and Ineff.gal3 siRNA) or galectin-3 siRNA (gal3 siRNA). Primary cilia were stained with antibody directed against acetylated-α-tubulin. Nuclei were detected by Hoechst 33342 staining. Scale bars, (A) 20 μm; (B) 10 μm; (C) lower magnifications, 10 μm. Higher magnifications (panels on the right side), 3 μm. (D) Primary cilium length was measured in 20 fields (20× objective) of postconfluent cells (day 4) from three independent experiments. Bars, mean ± SD. Statistical differences are presented (Mann-Whitney tests).

fluent MDCK cells. Furthermore, when we immunoprecipitated centrin-2, we found that galectin-3 was coprecipitated (Figure 5A). A similar result was obtained after immunoprecipitation of another major centrosome component, centrin-3 (data not shown). Interestingly, this association of galectin-3 to centrin-2 occurs between day 3 and 5, no significant

binding was detected before or after this time interval (Figure 5A). This was confirmed by the quantification of three independent experiments (Figure 5A). To verify that the galectin-3/centrin-2 interaction was effectively taking place within the centrosome, centrosomal fractions were prepared from MDCK cells harvested on day 3 and also on day 1 and
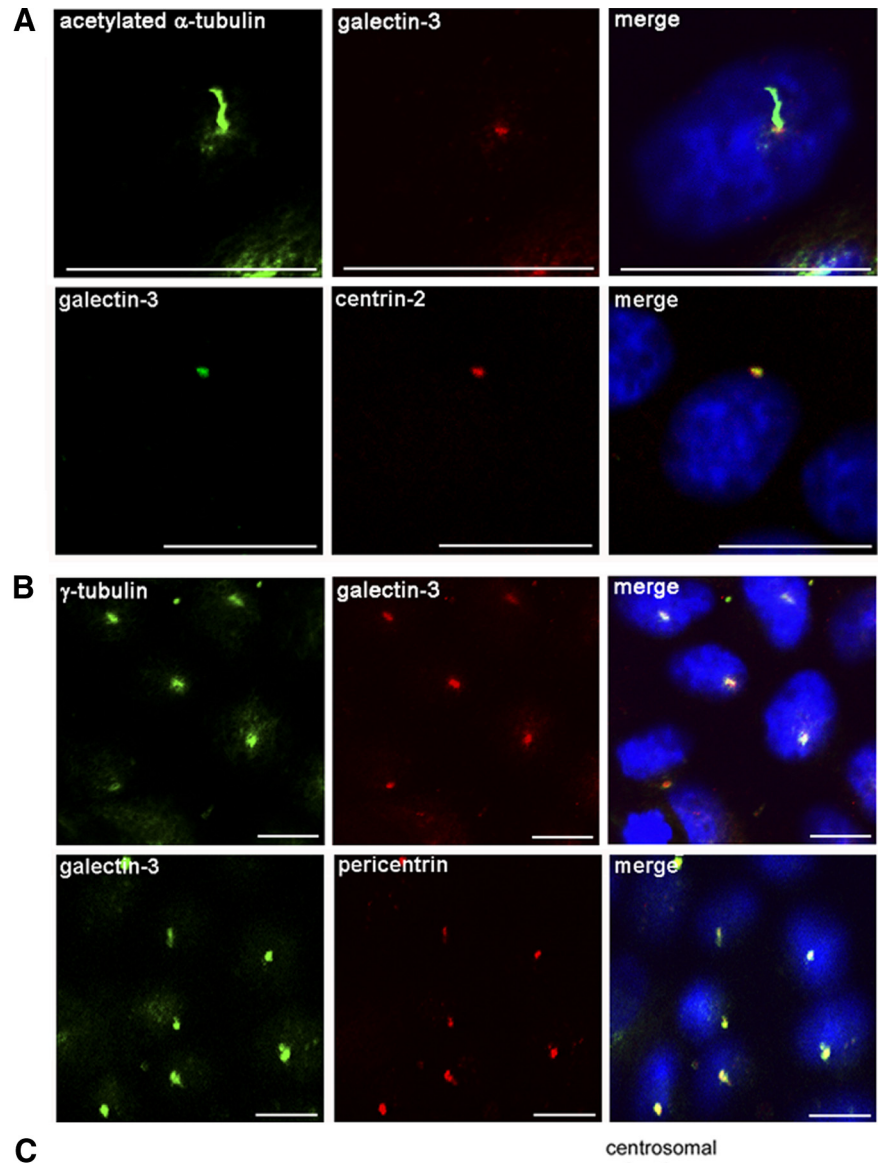
Figure 4. Galectin-3 is present at the centrosome of postconfluent MDCK cells. Double-immunostaining experiments with antibody directed against galectin-3 and against acetylated α-tubulin, centrin-2 (A), or γ-tubulin and pericentrin (B) MDCK cells after 3 d in monolayer cultures. Scale bars, 10 μm. (C) centrosomes were purified from day 3 MDCK cell cultures by density gradient centrifugation. Centrosomal fractions were identified based on the distribution of γ-tubulin and centrin-2. To test the purity of the preparations, the distribution of noncentrosomal proteins, such as flotillin-1, was also analyzed. PNS, postnuclear supernatant.

day 6 (Figure 5B). With each fraction, immunoprecipitation was performed with anti-centrin-2 antibody. Although centrin-2 could be readily detected in the centrosomal fractions obtained at each time point, galectin-3 was coprecipitated at day 3, but not at day 1 or day 6, thus confirming our previous observations. In summary, our data demonstrate that galectin-3 closely associates with the centrosome, but only during a limited period of time, when confluent MDCK cells initiate fine polarization process. It is worth noting that this is a different situation from that of cyst formation in which cyst expansion and cell polarization are continuous ongoing processes.
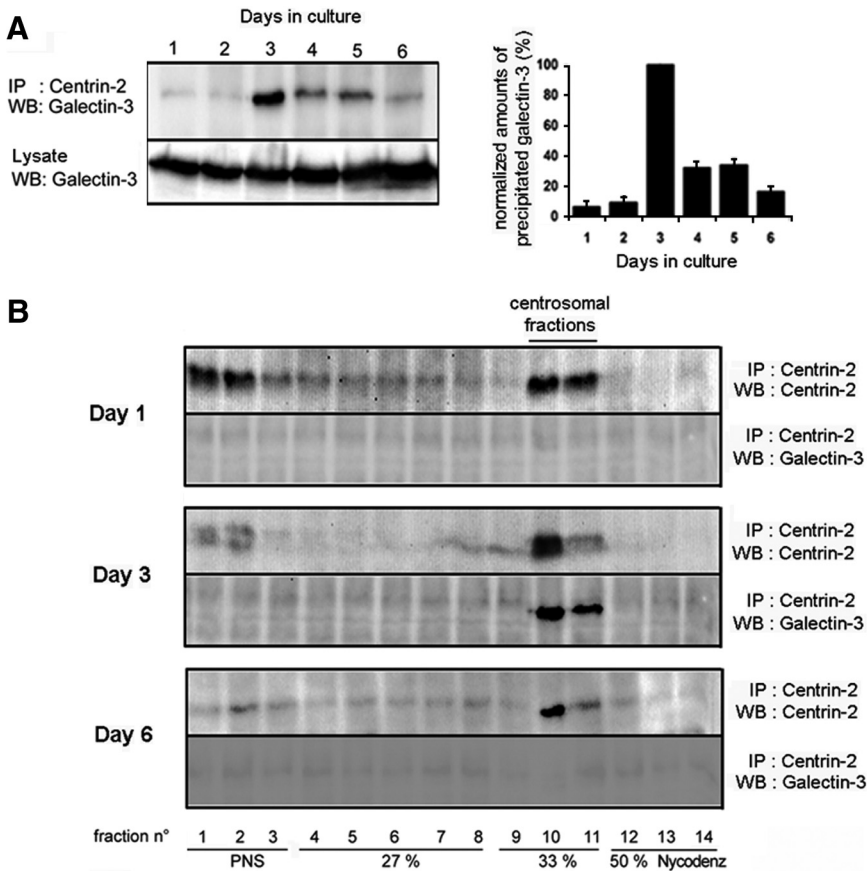
Figure 5. Galectin-3 transiently associates with the centrosome in MDCK cells. (A) Postnuclear supernatants (PNS) of MDCK cells, maintained in culture for different time points, were subjected to immunoprecipitation with centrin-2 antibody. The precipitated material was analyzed by immunoblot with anti-galectin-3 antibody. Crude lysates were loaded as controls for the expression level of galectin-3. Densitometric quantification of three representative immunoblot scans of galectin-3 copurified with centrin-2 are presented. (B) After centrosomal fractionation at different time points (days 1, 3, and 6), each gradient fraction was subjected to immunoprecipitation against centrin-2. Precipitates were analyzed by immunoblot with antibodies against centrin-2 and galectin-3.

Galectin-3 Silencing Leads to Centrosomal Abnormalities

This specific association of galectin-3 with centrosomes during cell polarization (Figures 4 and 5), together with the defects we observed in microtubule network (Figures 1 and 2 and Supplemental Figure 2C) and ciliary growth (Figure 3 and Supplemental Figure 2, D and E), led us to hypothesize that galectin-3 might be important for centrosome biology in renal cells. We thus examined the consequence of galectin-3 reduction on the distribution of centrosomes in MDCK cells. In postconfluent MDCK cells, most cells are quiescent, only a small fraction still divide with low frequency (Reinsch and Karsenti, 1994). Silencing of galectin-3 induced several centrosomal defects. First, an abnormal number of structures positive for the centrosomal markers, centrin-2 and pericentrin, was observed (Figure 6A, arrowheads, and Supplemental Figure 2F). Hence, a majority of control MDCK cells (80–90%) displayed one or two centrin-2–positive dots. In contrast, the majority of gal3 siRNA MDCK cells contained at least three centrin-2–positive foci. In fact, 40% of galectin-3–depleted cells had more than five centrin-2 aggregates (Figure 6B). Second, transfection of gal3 siRNA led to the formation of apparently larger centrosomal foci (Figure 6A, arrowheads). Measurement of their surface gave an estimate of ~40% increase in size (p < 0.01; n = 270; Figure 6C). Perturbation in the distribution of centrosomal markers was also observed in gal3 siRNA MDCK cysts. The reduction of galectin-3 led to the presence of supernumerary centrin-positive structures in the cytoplasm (Supplemental Figures 5 and 2G). In addition, we also noticed the frequent presence of unusual, long intracellular filaments, positive for centrosomal markers (Figure 6A, arrows, and Supplemental Figure 2F). These experiments showed that,

in MDCK cells, the down-regulation of galectin-3 directly interferes with the regulation in number, size, and shape of the centrosomes, implying a direct role for galectin-3 in centrosomal biology.

To test the validity of this conclusion in vivo, we compared the distribution of centrosomal markers in wt and *gal3−/−* mouse collecting ducts, which are quiescent cells (Figure 6D). In accordance with our in vitro data, strong abnormalities in the number and morphology of centrin-2–positive structures were detected in *galectin-3* null mutant mice. In wt cells (n = 6), centrin-2 staining revealed punctiform structures at the apical domain, facing the lumen of the tubule (Figure 6Da, arrowheads). In the mutant mice (n = 6), we observed a less regular centrin-2 staining pattern, with numerous positive structures dispersed inside all mutant cells (Figure 6Db, arrowheads). In severe cases, large centrin-2–positive aggregates were abnormally accumulated in the cytoplasm underneath the apical surface (Figure 6Dc). We also frequently noticed the presence of intracellular centrin-2–positive elongated structures (Figure 6D, b and c, arrows).

We further characterized these centrosomal abnormalities at the ultrastructural level. In wt collecting duct cells (n = 6), centrioles are generally detected as small electron-dense cylinders close by or anchored at the apical plasma membrane (Figure 7A). In *gal3−/−* collecting duct cells (n = 6; Figure 7B), we observed, in addition to these units, the appearance of many highly organized, atypical electron-dense aggregates, as well as very striking long intracellular filamentous structures, distinct from cilia. These filamentous structures display a mean diameter of 307 ± 70 nm and a length, varying according to the plane of ultrathin sections, from
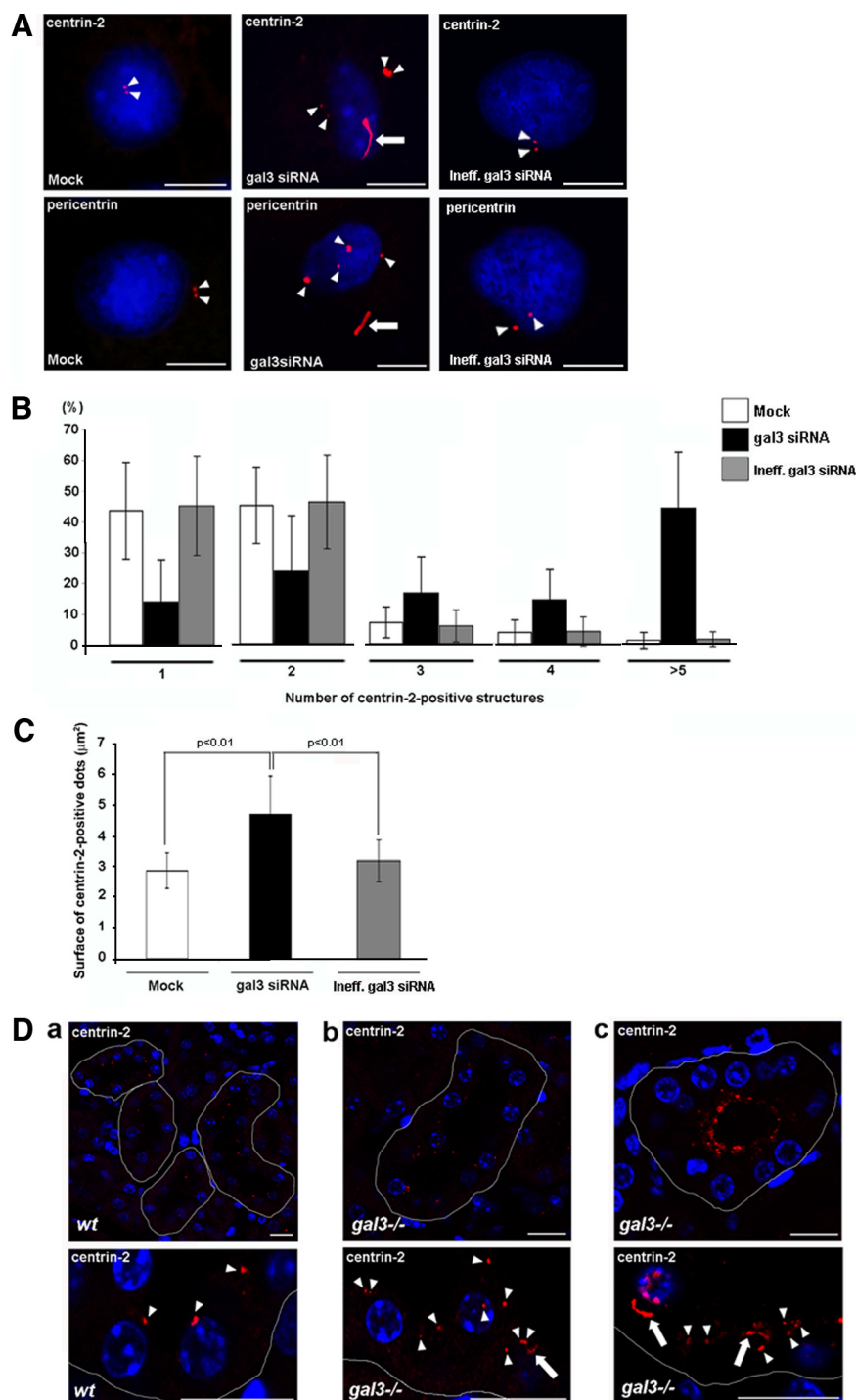
Figure 6. Depletion in galectin-3 leads to centrosomal abnormalities in vitro and in vivo. (A) Confocal analysis of the distribution of centrin-2 and pericentrin on day 3 MDCK cells transfected with control siRNAs (Mock and Ineff.gal3 siRNA) or galectin-3 siRNA (gal3 siRNA). Nuclei were detected by Hoechst 33342 staining. Arrowheads and arrows, centrin-2– or pericentrin-positive dots or intracellular filaments, respectively. Scale bars, 6 μm. Results were normalized. Centrin-2–positive foci were counted (B), and their surface was measured (C), in 20 40× fields of three independent experiments. White, black, and gray bars, Mock, gal3 siRNA and Ineff.gal3 siRNA cells, respectively. Bars, mean ± SD. Statistical differences are presented (Mann-Whitney tests). (D) confocal analysis of centrin-2 distribution in mouse collecting ducts from wt (a) or mutant tissue (b and c). Nuclei were detected by Hoechst 33342 staining. Tubules were delimited with a white line along basal membranes. Arrowheads and arrows, centrin-2– or pericentrin-positive dots or intracellular filaments, respectively. Bars, 10 μm.

0.70 to 9.5 μm (mean value 2.29 ± 2.1 μm). Given the density of these structures, it is very likely that they correspond to the elongated centrin-2–positive structures previously detected by confocal microscopy (Figure 6D). As shown in Figure 7C, immunostaining using a centrin-2 antibody on ultrathin sections revealed that these aberrant units in mutant cells (N = 3) were indeed positive for the centriolar marker, suggesting that these unusual units may arise from centrioles in absence of galectin-3. In summary, these in vitro and in vivo data demonstrate that the lack of galectin-3 influences centrosomal structures, which strongly argues in favor of a central role for galectin-3 in centrosome formation/stabilization.

DISCUSSION

In this study, we evaluated the participation of galectin-3 in renal morphogenesis. We found that galectin-3 is able to regulate cystogenesis and epithelial cell organization in MDCK cells grown in Matrigel, as previously shown in collagen matrix by Simons and colleagues (Torkko et al., 2008). Moreover, we showed that the absence of galectin-3
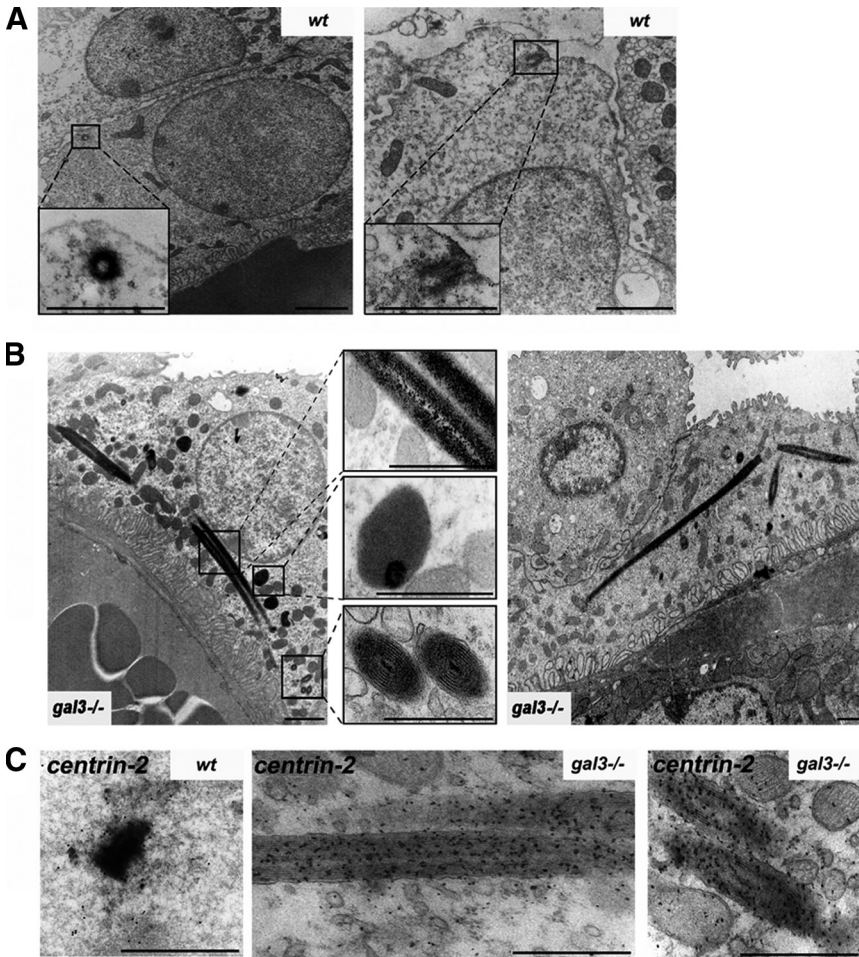
Figure 7. Loss of galectin-3 leads to the formation of aberrant centriolar-like structures in mouse *gal3*−/− kidneys. Ultrastructural analysis of centrioles in wt (A) or *galectin-3* null mutant (*gal3*−/−) (B) mouse collecting ducts. Bars, 1 μm. The insets show high magnifications of the regions in black boxes in A and B; bars, 0.5 μm. (C) Immunostaining for centrin-2 on *wt* or *gal3*−/− ultrathin sections. Antibody binding was visualized by incubation with a polyclonal anti-centrin-2 and 10-nm immunogold conjugated goat anti-rabbit IgG antibody; bars, 0.5 μm.

expression also perturbed the organization of collecting duct cells. Abnormalities in membrane compartmentation observed in these cells in vivo completely mirror the defects already reported in *gal3*−/− enterocytes (Delacour *et al.*, 2008). First, we observed the mislocalization of nonraft proteins. Second, there is also a redirection of structural non-glycosylated apical proteins, and this is associated with the formation of numerous interdigitations along basolateral membranes (not shown). These results led us to hypothesize that, beyond its role in intracellular trafficking, galectin-3 may also participate in epithelial morphogenetic events. To test this, we decided to scrutinize epithelial cells undergoing polarization process. We found that the intracellular localization of the lectin is very dynamic during the process of MDCK cell differentiation. Interestingly, once the cells have reached confluency, galectin-3 relocates at the centrosome, a cell organizing center (Musch, 2004; Luders and Stearns, 2007; Bornens, 2008). A centrosomal association of galectin-3 was previously detected by Chiu *et al.* (2006).

In addition, we observed that galectin-3 colocalizes with several centrosomal and centriolar markers and that galectin-3 is present in preparations of centrosomes from MDCK cells, where it can be copurified with centrin-2, a centriolar protein. Although the exact nature of these interactions remains to be elucidated, these data show a tight association of galectin-3 with the centrosome. In MDCK cells lacking galectin-3, there were supranumerous centrosomal structures, suggesting a possible role of the protein either in centriole duplication or in centriole segregation during cytokinesis.

Moreover, there were also striking abnormalities in centrosome shape and size. We also noticed frequent and remarkable long filaments, positive for centriolar components inside MDCK cells transfected with galectin-3 siRNA and in *gal3*−/− epithelial kidney cells. These unusual long filamentous structures may be related to those recently described by Spektor *et al.* (2007) or Sandvig and colleagues (Kuriyama *et al.*, 2009). However, ultrastructural analyses on *gal3*−/− kidney cells revealed that the long intracellular filaments have no clear surrounding membranes and do not exhibit the classical microtubular 9+0 organization. As these are two key features of ciliated structures, it seems likely that these long filaments and aggregates result from aberrant polymerization of centrosomal components. How the lack of galectin-3 triggers these effects warrants further investigations. One piece of information comes from the kinetic analysis carried out on polarizing MDCK cells in which we showed that galectin-3 is only transiently associated with the centrosome, indicating that it might be a regulating factor rather than a constitutive core component. One possibility could be that galectin-3 already plays a role in protein trafficking at this early step of cell differentiation and thus ensures the targeting of key regulators at the centrosome and basal bodies. However, it could play a totally different function. For instance, it could be stabilizing the centrosomal/basal body structure. Alternatively, it might be acting at the level of the microtubules and modulating nucleation processes.

In the course of this study, we showed that consequences of galectin-3 absence on centrosomes are concomitant with

abnormalities at the level of the microtubules and of the primary cilia. We first observed severe perturbations of microtubule network in the absence of galectin-3 both in vitro and in vivo. As centrosomes are microtubule-nucleating and -organizing centers (Luders and Stearns, 2007), it is likely that the misorganization of microtubules is due to the absence of galectin-3 in centrosomes. Furthermore, the integrity of microtubule network is required not only for epithelial cell shape, but also for epithelial polarity with correct lumen formation and stabilization (Cohen *et al.,* 2004; Musch, 2004). This is well illustrated in the case of ischemia-reperfusion experiments. After chemical anoxia in vitro or renal ischemia-reperfusion in rat, the loss of epithelial polarity is accompanied by the delocalization of the centrosome and a profound misorganization of the microtubular network (Wald *et al.,* 2003). Interestingly, this physiological stress provokes defects of membrane compartimentation: pseudolumenal faces form along basolateral membranes of renal cells, brush border components mislocalize, and regular membrane interdigitations, similar to microvilli, appear laterally (Brown *et al.,* 1997). This phenomenon is not restricted to renal cells. In rat and mouse enterocytes, colchicine-induced microtubule perturbation also induces the mislocalization of villin together with the formation of microvilli-like structures along basolateral membranes (Achler *et al.,* 1989). These defects are remarkably reminiscent of those found in galectin-3 null mutant enterocytes (Delacour *et al.,* 2008) and renal cells (Figure 2 and 7). Taken together, we propose that the defects we observed in cell polarization could result from perturbations in the microtubular architecture, at least in part.

Epithelial morphogenesis also relies on a functional primary cilium, an organelle originating from subapical centrioles (Azimzadeh and Bornens, 2007; Dawe *et al.,* 2007; Satir and Christensen, 2007). Primary cilium defects have been clearly identified as causal events, responsible for major abnormalities in the organization of epithelial cells, for instance characteristic of the development of the autosomal recessive polycystic kidney disease (APKD; Singla and Reiter, 2006; Kolb and Nauli, 2008). An association of galectin-3 with the primary cilium was reported, but this observation was not further pursued (Winyard *et al.,* 1997; Chiu *et al.,* 2006). Here, we found that galectin-3 specifically locates at the base of the primary cilium. We show that, upon galectin-3 silencing, primary cilium development was disturbed, with the generation of longer and dysmorphic cilia. To our knowledge, such cilium abnormalities are quite unusual. Most reports describe either the absence of primary cilium or the formation of stunted cilia. For example, a study performed in *Caenorhabditis elegans* showed that mutations in nephrocystin genes (NH-1 and -4) led to the formation of misshaped cilia, i.e., longer and curly cilia (Jauregui *et al.,* 2008). Interestingly, abnormally long primary cilia have now been found on mouse kidney epithelial cells in response to tubular injury (Verghese *et al.,* 2009). These results suggest that the lack of galectin-3 induces a state of chronic renal stress.

Altogether, these data show that the absence of galectin-3 influences the stabilization of centrosomes and primary cilia, with effects on epithelial cell organization. As a consequence, one might expect more severe phenotypes in mutant mice. But, adult *gal3*−/− mice kept in animal house conditions are alive, do not display any major phenotypes, and only exhibit mild abnormalities (Colnot *et al.,* 1998, 2001; Liu *et al.,* 2002; Bichara *et al.,* 2006). In the future, it will be important to study the recovery potential of mutant epithelial cells after renal ischemia or even kidney reduction (Molitoris,

1998; Sheridan and Bonventre, 2000; Pillebout *et al.,* 2001; Lautrette *et al.,* 2005). In this context, Winyard and coworkers have already demonstrated that the loss of galectin-3 enhances the severity of the polycystic kidney phenotype. Using the *cpk* mouse model (congenital polycystic kidney), which shares similarities with APKD, they showed that *cpk;gal3*−/− mice exhibit a higher tendency in renal cyst formation than *cpk;gal3*+/+ (Chiu *et al.,* 2006).

In addition, the importance of centrosomes in organism development is currently in debate. For instance, recent studies carried out in *Drosophila* demonstrated that centrosomal amplification have no drastic consequence on fly viability (Basto *et al.,* 2006; Basto *et al.,* 2008). But, when such mutant cells with supranumerous centrosomes are transplanted to wt flies, they induce the development of metastatic tumors (Basto *et al.,* 2008). In fact, centrosomal aberrations are a potential source of genetic instability and perturbation of epithelial homeostasis, such abnormalities are frequently observed in early steps of carcinogenesis (Fukasawa, 2005; Nigg, 2006). It is worth noting that defects in galectin-3 expression or cellular localization are frequently reported in epithelial cancers (Califice *et al.,* 2004). It would be interesting to explore a potential relationship between these observations and the role of galectin-3 in centrosome biology.

Galectin-3 belongs to a family of secreted proteins, which do not possess signal peptide, and thus bypass the classical secretion mechanisms. Although this mechanism is unknown, it nevertheless appears to be a highly regulated process (Nickel, 2003, 2005). In addition, galectin-3 is found associated with numerous intracellular organelles such as the nucleus, mitochondria, endosomes, carrier vesicles, and now the centrosome, depending on the cell type, the cell cycle or even the cell differentiation (Liu *et al.,* 2002; Nickel, 2003; Delacour *et al.,* 2009). Although it is not possible to reach an integrated picture at this stage, it is however clear that understanding the signals that induce the shifts in galectin-3 distribution constitutes a major challenge in the field.

ACKNOWLEDGMENTS

REFERENCES

Achler, C., Filmer, D., Merte, C., and Drenckhahn, D. (1989). Role of microtubules in polarized delivery of apical membrane proteins to the brush border of the intestinal epithelium. J. Cell Biol. *109,* 179–189.

Assemat, E., Bazellieres, E., Pallesi-Pocachard, E., Le Bivic, A., and Massey-Harroche, D. (2008). Polarity complex proteins. Biochim. Biophys. Acta *1778,* 614–630.

Azimzadeh, J., and Bornens, M. (2007). Structure and duplication of the centrosome. J. Cell Sci. *120,* 2139–2142.

Barondes, S. H., Cooper, D. N., Gitt, M. A., and Leffler, H. (1994). Galectins. Structure and function of a large family of animal lectins. J. Biol. Chem. *269,* 20807–20810.

Basto, R., Brunk, K., Vinadogrova, T., Peel, N., Franz, A., Khodjakov, A., and Raff, J. W. (2008). Centrosome amplification can initiate tumorigenesis in flies. Cell *133,* 1032–1042.

Basto, R., Lau, J., Vinogradova, T., Gardiol, A., Woods, C. G., Khodjakov, A., and Raff, J. W. (2006). Flies without centrioles. Cell *125,* 1375–1386.

Bichara, M., *et al.* (2006). Exploring the role of galectin 3 in kidney function: a genetic approach. Glycobiology *16*, 36–45.

Bonilha, V. L., Finnemann, S. C., and Rodriguez-Boulan, E. (1999). Ezrin promotes morphogenesis of apical microvilli and basal infoldings in retinal pigment epithelium. J. Cell Biol. *147*, 1533–1548.

Bornens, M. (2008). Organelle positioning and cell polarity. Nat. Rev. *9*, 874–886.

Bornens, M., and Moudjou, M. (1999). Studying the composition and function of centrosomes in vertebrates. Methods Cell Biol. *61*, 13–34.

Brown, D., Lee, R., and Bonventre, J. V. (1997). Redistribution of villin to proximal tubule basolateral membranes after ischemia and reperfusion. Am. J. Physiol. *273*, F1003–F1012.

Califice, S., Castronovo, V., and Van Den Brule, F. (2004). Galectin-3 and cancer (Review). Int. J. Oncol. *25*, 983–992.

Chiu, M. G., *et al.* (2006). Galectin-3 associates with the primary cilium and modulates cyst growth in congenital polycystic kidney disease. Am. J. Pathol. *169*, 1925–1938.

Cohen, D., Brennwald, P. J., Rodriguez-Boulan, E., and Musch, A. (2004). Mammalian PAR-1 determines epithelial lumen polarity by organizing the microtubule cytoskeleton. J. Cell Biol. *164*, 717–727.

Colnot, C., Fowlis, D., Ripoche, M. A., Bouchaert, I., and Poirier, F. (1998). Embryonic implantation in galectin 1/galectin 3 double mutant mice. Dev. Dyn. *211*, 306–313.

Colnot, C., Sidhu, S. S., Balmain, N., and Poirier, F. (2001). Uncoupling of chondrocyte death and vascular invasion in mouse galectin 3 null mutant bones. Dev. Biol. *229*, 203–214.

Cooper, D. N. (2002). Galectinomics: finding themes in complexity. Biochim. Biophys. Acta *1572*, 209–231.

Crepaldi, T., Gautreau, A., Comoglio, P. M., Louvard, D., and Arpin, M. (1997). Ezrin is an effector of hepatocyte growth factor-mediated migration and morphogenesis in epithelial cells. J. Cell Biol. *138*, 423–434.

Dawe, H. R., Farr, H., and Gull, K. (2007). Centriole/basal body morphogenesis and migration during ciliogenesis in animal cells. J. Cell Sci. *120*, 7–15.

Delacour, D., Cramm-Behrens, C. I., Drobecq, H., Le Bivic, A., Naim, H. Y., and Jacob, R. (2006). Requirement for galectin-3 in apical protein sorting. Curr. Biol. *16*, 408–414.

Delacour, D., *et al.* (2005). Galectin-4 and sulfatides in apical membrane trafficking in enterocyte-like cells. J. Cell Biol. *169*, 491–501.

Delacour, D., Greb, C., Koch, A., Salomonsson, E., Leffler, H., Le Bivic, A., and Jacob, R. (2007). Apical sorting by galectin-3-dependent glycoprotein clustering. Traffic *8*, 379–388.

Delacour, D., Koch, A., Ackermann, W., Eude-Le Parco, I., Elsasser, H. P., Poirier, F., and Jacob, R. (2008). Loss of galectin-3 impairs membrane polarisation of mouse enterocytes in vivo. J. Cell Sci. *121*, 458–465.

Delacour, D., Koch, A., and Jacob, R. (2009). The role of galectins in protein trafficking. Traffic *10*, 1405–1413.

Dictenberg, J. B., Zimmerman, W., Sparks, C.A., Young, A., Vidair, C., Zheng, Y., Carrington, W., Fay, F. S., and Doxsey, S. J. (1998). Pericentrin and gamma-tubulin form a protein complex and are organized into a novel lattice at the centrosome. J. Cell Biol. *141*, 163–174.

Elola, M. T., Wolfenstein-Todel, C., Troncoso, M. F., Vasta, G. R., and Rabinovich, G. A. (2007). Galectins: matricellular glycan-binding proteins linking cell adhesion, migration, and survival. Cell Mol. Life Sci. *64*, 1679–1700.

Fliegauf, M., Benzing, T., and Omran, H. (2007). When cilia go bad: cilia defects and ciliopathies. Nat. Rev. *8*, 880–893.

Fukasawa, K. (2005). Centrosome amplification, chromosome instability and cancer development. Cancer Lett. *230*, 6–19.

Hughes, R. C. (1999). Secretion of the galectin family of mammalian carbohydrate-binding proteins. Biochim. Biophys. Acta *1473*, 172–185.

Hughes, R. C. (2001). Galectins as modulators of cell adhesion. Biochimie *83*, 667–676.

Jauregui, A. R., Nguyen, K. C., Hall, D. H., and Barr, M. M. (2008). The *Caenorhabditis elegans* nephrocystins act as global modifiers of cilium structure. J. Cell Biol. *180*, 973–988.

Kamsteeg, E. J., Duffield, A. S., Konings, I. B., Spencer, J., Pagel, P., Deen, P. M., and Caplan, M. J. (2007). MAL decreases the internalization of the aquaporin-2 water channel. Proc. Natl. Acad. Sci. USA *104*, 16696–16701.

Kim, H., Lee, J., Hyun, J. W., Park, J. W., Joo, H. G., and Shin, T. (2007). Expression and immunohistochemical localization of galectin-3 in various mouse tissues. Cell Biol. Int. *31*, 655–662.

Kolb, R. J., and Nauli, S. M. (2008). Ciliary dysfunction in polycystic kidney disease: an emerging model with polarizing potential. Front. Biosci. *13*, 4451–4466.

Krzeslak, A., and Lipinska, A. (2004). Galectin-3 as a multifunctional protein. Cell. Mol. Biol. Lett. *9*, 305–328.

Kuriyama, R., Bettencourt-Dias, M., Hoffmann, I., Arnold, M., and Sandvig, L. (2009). Gamma-tubulin-containing abnormal centrioles are induced by insufficient Plk4 in human HCT116 colorectal cancer cells. J. Cell Sci. *122*, 2014–2023.

Laoukili, J., Perret, E., Middendorp, S., Houcine, O., Guennou, C., Marano, F., Bornens, M., and Tournier, F. (2000). Differential expression and cellular distribution of centrin isoforms during human ciliated cell differentiation in vitro. J. Cell Sci. *11*(Pt 8), 1355–1364.

Lautrette, A., Li, S., Alili, R., Sunnarborg, S. W., Burtin, M., Lee, D. C., Friedlander, G., and Terzi, F. (2005). Angiotensin II and EGF receptor crosstalk in chronic kidney diseases: a new therapeutic approach. Nat. Med. *11*, 867–874.

Lindstedt, R., Apodaca, G., Barondes, S. H., Mostov, K. E., and Leffler, H. (1993). Apical secretion of a cytosolic protein by Madin-Darby canine kidney cells. Evidence for polarized release of an endogenous lectin by a nonclassical secretory pathway. J. Biol. Chem. *268*, 11750–11757.

Liu, F. T., Patterson, R. J., and Wang, J. L. (2002). Intracellular functions of galectins. Biochim. Biophys. Acta *1572*, 263–273.

Liu, F. T., and Rabinovich, G. A. (2005). Galectins as modulators of tumour progression. Nat. Rev. Cancer *5*, 29–41.

Luders, J., and Stearns, T. (2007). Microtubule-organizing centres: a re-evaluation. Nat. Rev. *8*, 161–167.

Martin-Belmonte, F., and Mostov, K. (2008). Regulation of cell polarity during epithelial morphogenesis. Curr. Opin. Cell Biol. *20*, 227–234.

Molitoris, B. A. (1998). Ischemic acute renal failure: exciting times at our fingertips. Curr. Opin. Nephrol. Hypertens. *7*, 405–406.

Musch, A. (2004). Microtubule organization and function in epithelial cells. Traffic *5*, 1–9.

Nickel, W. (2003). The mystery of nonclassical protein secretion. A current view on cargo proteins and potential export routes. Eur J. Biochem. *270*, 2109–2119.

Nickel, W. (2005). Unconventional secretory routes: direct protein export across the plasma membrane of mammalian cells. Traffic *6*, 607–614.

Nigg, E.A. (2006). Origins and consequences of centrosome aberrations in human cancers. Int. J. Cancer *119*, 2717–2723.

O'Brien, L. E., Zegers, M. M., and Mostov, K. E. (2002). Opinion: Building epithelial architecture: insights from three-dimensional culture models. Nat. Rev. *3*, 531–537.

Pillebout, E., Burtin, M., Yuan, H. T., Briand, P., Woolf, A. S., Friedlander, G., and Terzi, F. (2001). Proliferation and remodeling of the peritubular microcirculation after nephron reduction: association with the progression of renal lesions. Am. J. Pathol. *159*, 547–560.

Poirier, F. (2002). Roles of galectins in vivo. Biochem. Soc. Symp. *95–103*.

Rabinovich, G. A., Rubinstein, N., and Toscano, M. A. (2002). Role of galectins in inflammatory and immunomodulatory processes. Biochim. Biophys. Acta *1572*, 274–284.

Reinsch, S., and Karsenti, E. (1994). Orientation of spindle axis and distribution of plasma membrane proteins during cell division in polarized MDCKII cells. J. Cell Biol. *126*, 1509–1526.

Revenu, C., Athman, R., Robine, S., and Louvard, D. (2004). The co-workers of actin filaments: from cell structures to signals. Nat. Rev. *5*, 635–646.

Satir, P., and Christensen, S. T. (2007). Overview of structure and function of mammalian cilia. Annu. Rev. Physiol. *69*, 377–400.

Satir, P., and Christensen, S. T. (2008). Structure and function of mammalian cilia. Histochem. Cell Biol. *129*, 687–693.

Sheridan, A. M., and Bonventre, J. V. (2000). Cell biology and molecular mechanisms of injury in ischemic acute renal failure. Curr. Opin. Nephrol. Hypertens. *9*, 427–434.

Singla, V., and Reiter, J. F. (2006). The primary cilium as the cell's antenna: signaling at a sensory organelle. Science *313*, 629–633.

Spektor, A., Tsang, W. Y., Khoo, D., and Dynlacht, B. D. (2007). Cep97 and CP110 suppress a cilia assembly program. Cell *130*, 678–690.

Tanos, B., and Rodriguez-Boulan, E. (2008). The epithelial polarity program: machineries involved and their hijacking by cancer. Oncogene *27,* 6939–6957.

Torkko, J. M., Manninen, A., Schuck, S., and Simons, K. (2008). Depletion of apical transport proteins perturbs epithelial cyst formation and ciliogenesis. J. Cell Sci. *121,* 1193–1203.

Verghese, E., Ricardo, S. D., Weidenfeld, R., Zhuang, J., Hill, P. A., Langham, R. G., and Deane, J. A. (2009). Renal primary cilia lengthen after acute tubular necrosis. J. Am. Soc. Nephrol. *20,* 2147–2153.

Wald, F. A., Figueroa, Y., Oriolo, A. S., and Salas, P. J. (2003). Membrane repolarization is delayed in proximal tubules after ischemia-reperfusion: possible role of microtubule-organizing centers. Am. J. Physiol. *285,* F230–F240.

Winyard, P. J., Bao, Q., Hughes, R. C., and Woolf, A. S. (1997). Epithelial galectin-3 during human nephrogenesis and childhood cystic diseases. J. Am. Soc. Nephrol. *8,* 1647–1657.

Yu, M. J., Pisitkun, T., Wang, G., Aranda, J. F., Gonzales, P. A., Tchapyjnikov, D., Shen, R. F., Alonso, M. A., and Knepper, M. A. (2008). Large-scale quantitative LC-MS/MS analysis of detergent-resistant membrane proteins from rat renal collecting duct. Am. J. Physiol. Cell Physiol. *295,* C661–C678.